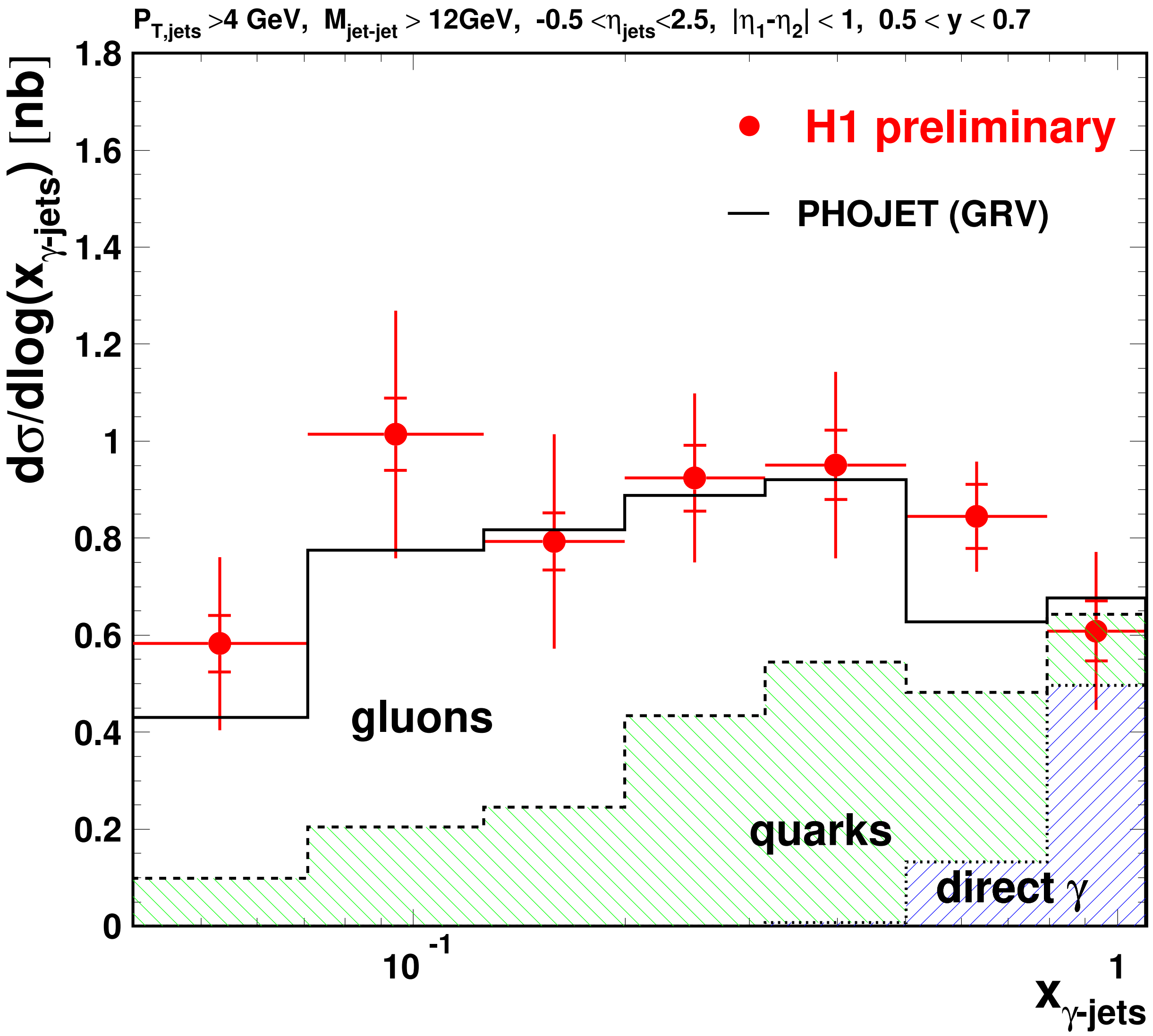

Figure 1: The measured di-jet cross section in photoproduction processes at HERA as function of x_γ. The jets were found with the CDFCONE-algorithm ($R = 0.7$). The data are compared to the LO QCD calculation of PHOJET with the GRV-LO parton density functions for the photon and proton and E_T for the factorisation and renormalisation scale. Also indicated are the different contributions of direct photon processes and resolved photon processes, where either quarks or gluons contribute.

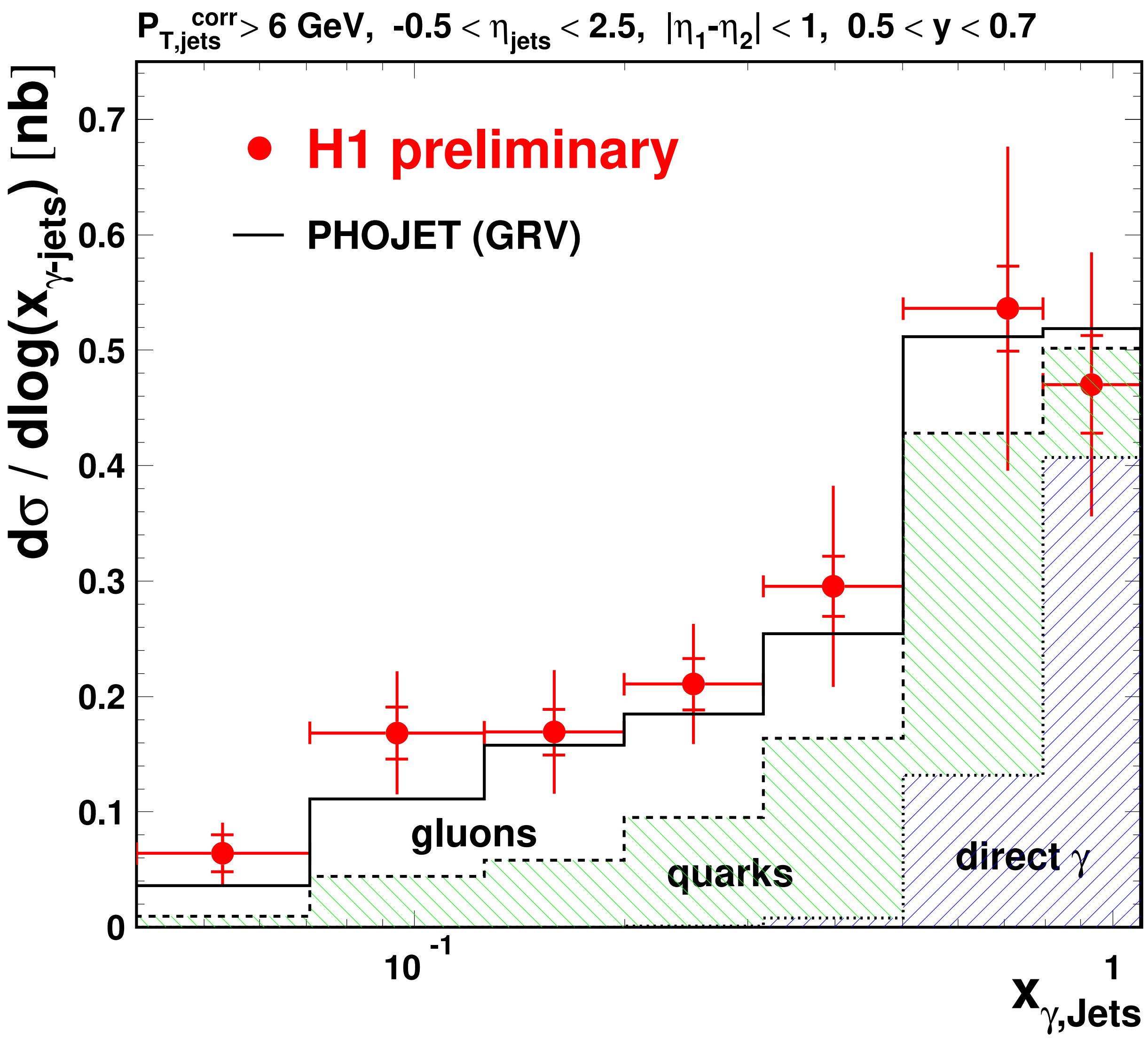

Figure 2: The measured di-jet cross section in photoproduction processes at HERA as function of x_γ. The jets were found with the CDFCONE-algorithm ($R = 0.7$). The transverse energy of the jets was required to be greater than 6 GeV after correcting for pedestal energy due to the underlying event. The data are compared to the LO QCD calculation of PHOJET with the GRV-LO parton density functions for the photon and proton and E_T for the factorisation and renormalisation scale. Also indicated are the different contributions of direct photon processes and resolved photon processes, where either quarks or gluons contribute.

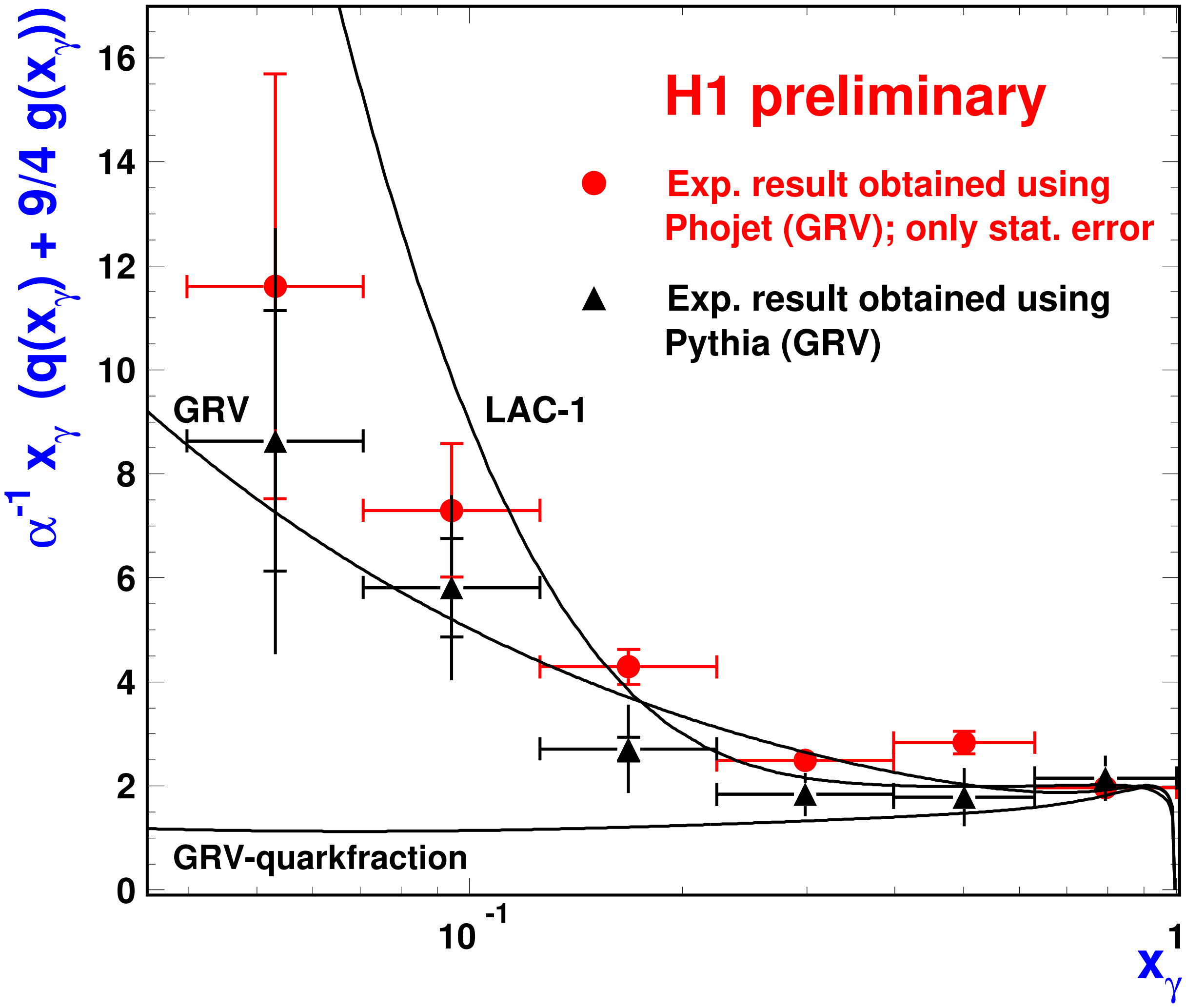

Figure 3: Effective parton densities of the photon as function of x_γ for a mean $P_t^2 = 74$ GeV^2 of the hard partons. The effective parton densities were determined from di-jet photoproduction events recorded with the H1-detector in 1996 using the PHOJET-model (circles; just statistical error) and the PYTHIA-model (triangles; statistical and exp. systematical errors added in quadrature) for the unfolding procedure. For the factorisation and renormalisation scale in the models P_T of the hard partons was used. Shown are also the GRV-LO and LAC-1 parton density parameterisations. Also indicated is the fraction of the quark density of the photon which contributes to the effective partondensity of the photon.

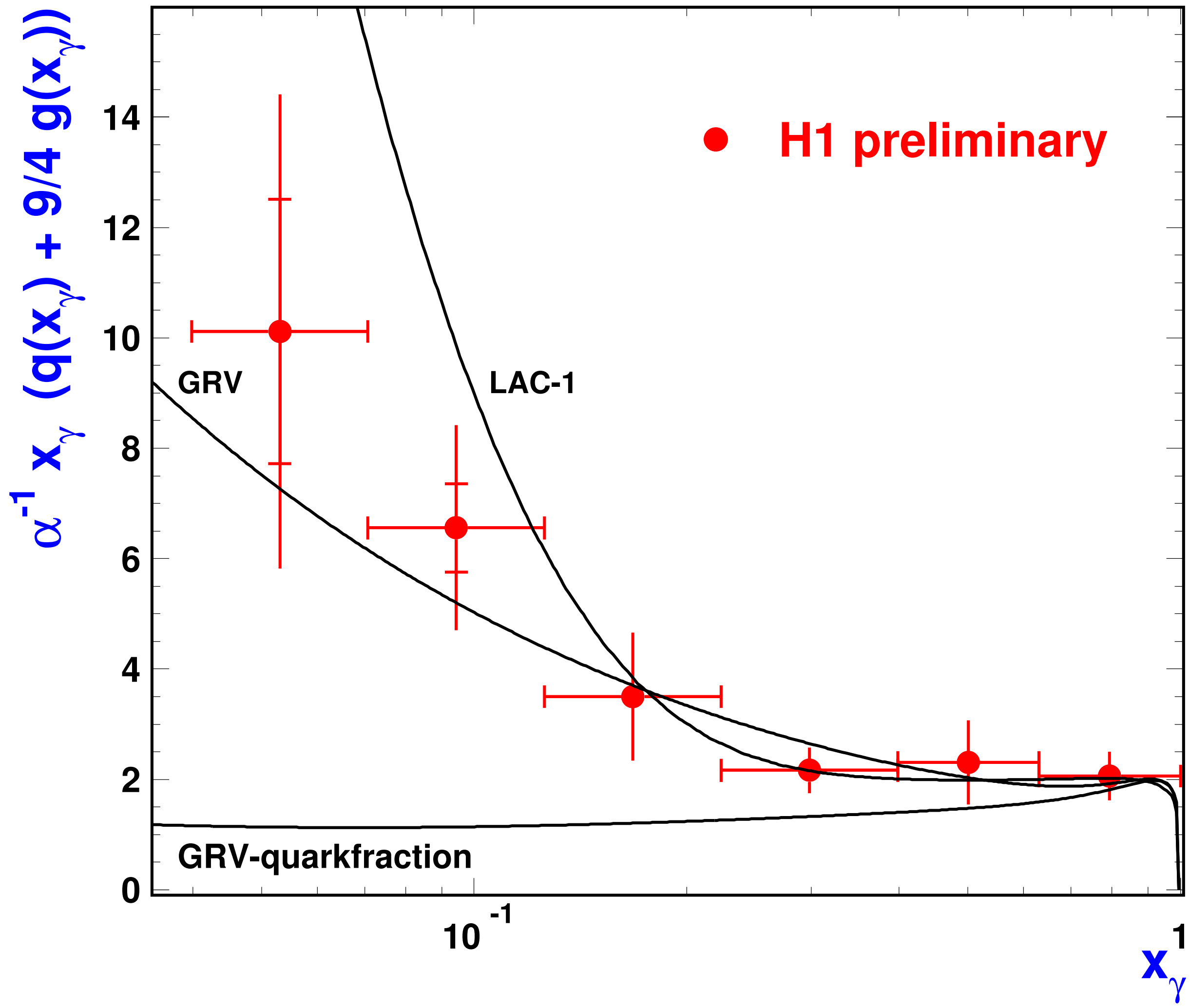

Figure 4: Effective parton density of the photon as function of x_γ for a mean $P_t^2 = 74$ GeV^2 of the hard partons. The effective parton density was determined from di-jet photoproduction events recorded with the H1-detector in 1996. Shown are also the GRV-LO and LAC-1 parton density parameterisations. Also indicated is the fraction of the quark density of the photon which contributes to the effective partondensity of the photon.

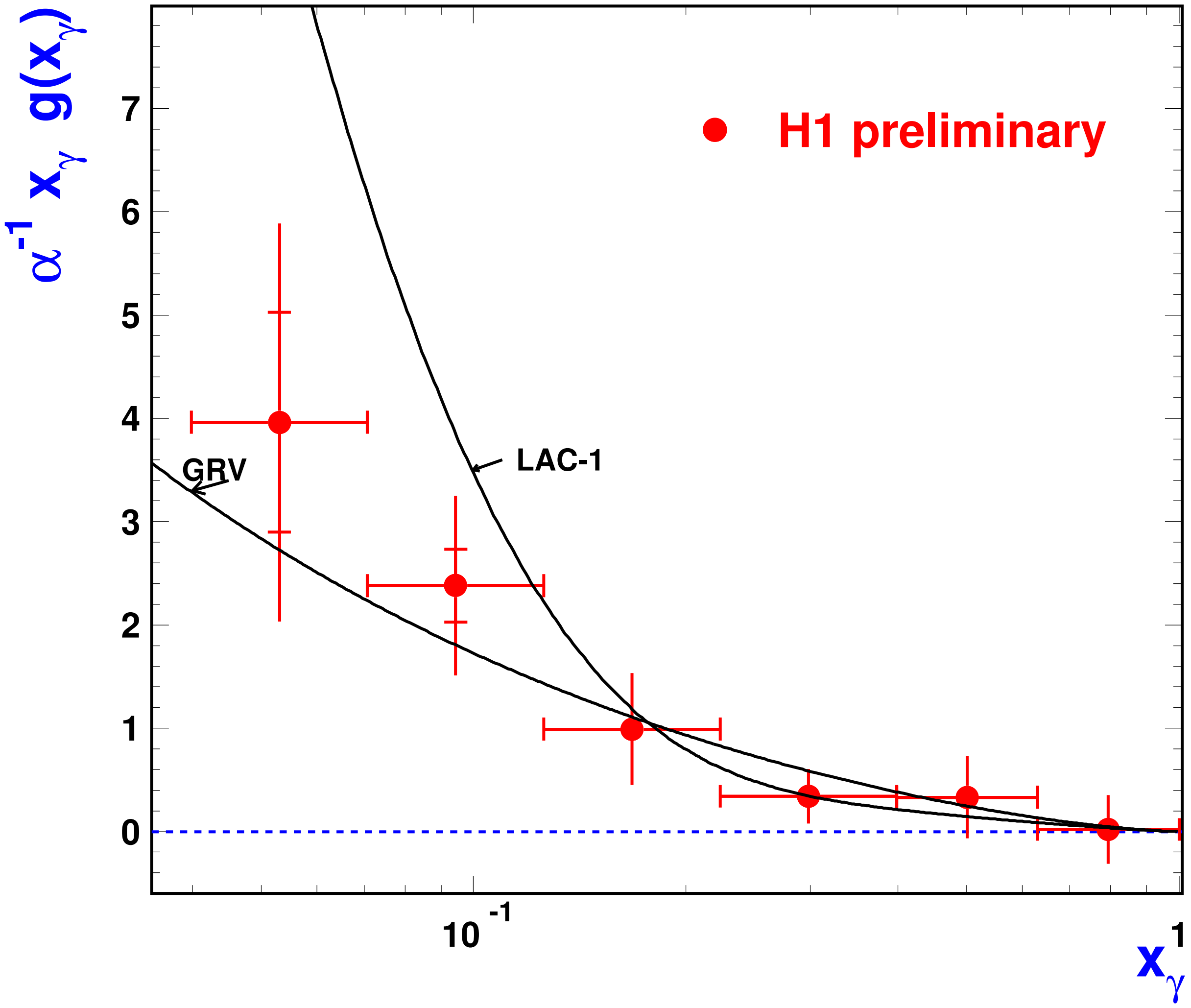

Figure 5: Gluon density of the photon as function of x_γ for a mean $P_t^2 = 74$ GeV^2 of the hard partons. The gluon density was determined from di-jet photoproduction events recorded with the H1-detector in 1996. Shown are also the GRV-LO and LAC-1 parton density parameterisations.

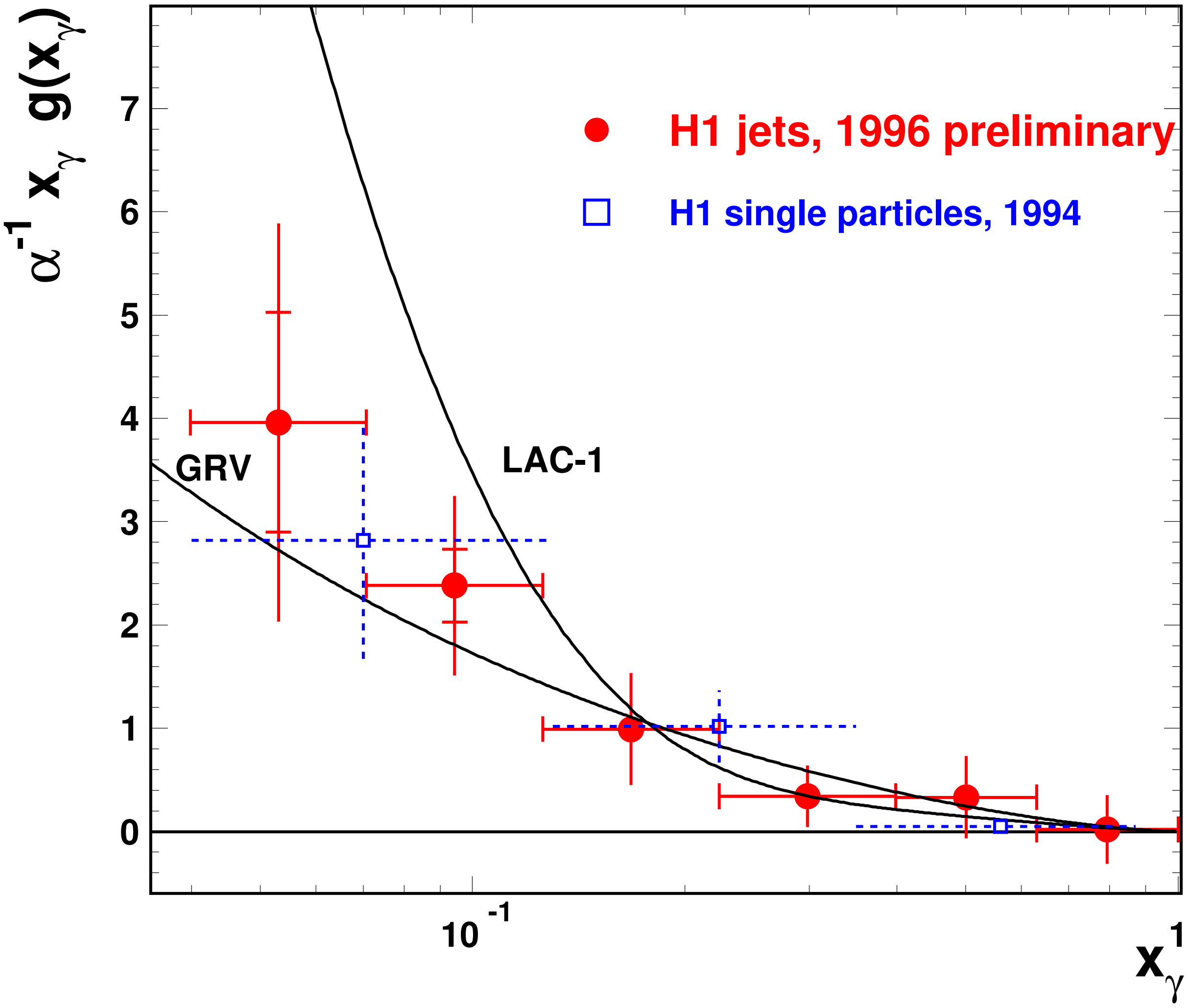

Figure 6: Comparison of the gluon density determined from di-jet photoproduction events taken in 1996 with earlier measurements of H1. Shown are also the GRV-LO and LAC-1 parton density parameterisations.